

# Dual-wavelength laser annealing

D. H. Auston and J. A. Golovchenko

*Bell Laboratories, Murray Hill, New Jersey 07974*

T. N. C. Venkatesan

*Bell Laboratories, Crawford Hill, New Jersey 07733*

(Received 15 January 1979; accepted for publication 19 February 1979)

A simple and efficient method of annealing ion-implantation damage in semiconductors is demonstrated which utilizes a relatively weak optical pulse in the visible to initiate surface melting in combination with a more energetic infrared pulse to drive in the melt front to the crystalline substrate. The efficacy of this approach is illustrated by an example in which an arsenic-implanted silicon crystal is simultaneously exposed to 530- and 1060-nm pulses. The results are discussed in relation to theoretical estimates of the melting thresholds at the two wavelengths.

PACS numbers: 81.40.Ef, 42.60. — v

Laser annealing<sup>1</sup> has been demonstrated to be an effective method of restoring the crystallinity of semiconductors which have been rendered amorphous by ion implantation. Two distinctly different annealing mechanisms have been identified. In the first case, the laser is used to heat the material to an elevated temperature without melting and regrowth occurs by solid-phase epitaxy<sup>2</sup> similar to conventional oven annealing. The other method uses more intense pulses of short duration to melt<sup>3</sup> the entire amorphous layer, and regrowth then occurs by liquid-phase epitaxy with the underlying crystalline substrate acting as the seed. The latter approach usually employs *Q*-switched solid-state lasers. For efficient annealing it is desirable to use a wavelength of excitation which is strongly absorbed, which for most semiconductors requires the use of visible or shorter wavelengths. Unfortunately, the most readily available and reliable *Q*-switched lasers are the neodymium lasers which emit in the infrared at 1060 nm. Although these lasers have been successfully used for annealing,<sup>1</sup> the threshold energies are high and depend strongly on the implant dose. It is also more difficult to obtain uniform anneals.<sup>4</sup> Recent measurements,<sup>5</sup> for example, show that the thresholds for melting a silicon wafer implanted with  $10^{15}$  arsenic atoms/cm<sup>2</sup> at 30 keV are 0.21 and 3.7 J/cm<sup>2</sup> at 530 and 1060 nm, respectively. Although second-harmonic generation can be used to convert infrared emission into the visible, it is difficult to achieve efficiencies greater than 30% with high-energy systems.

In this paper, we describe a simple and efficient approach to laser annealing which utilizes two optical pulses. A relatively weak visible pulse is used to initiate surface melting, and the melt front is then driven in by a more energetic infrared pulse. The key feature of this approach is the recognition that the optical properties of liquid semiconductors are metallic<sup>6</sup> and hence absorb infrared light with essentially the same efficiency as visible light. The large difference in melting thresholds between the infrared and visible wavelengths is due entirely to the much weaker infrared absorption in the solid phase. Once melting, the semiconductor is essentially color blind. Hence, it is necessary to use only as

much visible light as is necessary to produce melting of a surface layer to a depth of only one optical skin depth (approximately 100 Å for liquid silicon). The infrared light will then be strongly absorbed and can drive the melt front through the entire amorphous layer to the crystalline substrate.

An example is illustrated in Fig. 1. A *Q*-switched Nd : glass laser-amplifier system was used to generate an infrared (1060 nm) pulse of 1.75 J having a duration of 40 ns and a diameter of 8 mm in a single transverse mode. A KDP crystal was used to produce a weaker harmonic (530 nm) pulse of 0.085 J having a duration of 30 ns and a diameter of 6 mm. A  $\langle 100 \rangle$  silicon wafer was implanted at 30 keV with  $10^{15}$  arsenic atoms/cm<sup>3</sup> producing an amorphous layer 480 Å thick. The effect of the pulses on the silicon wafer was monitored by time-resolved reflectivity. This technique, which has previously been described in detail,<sup>3</sup> enables a direct measurement of the duration of the liquid phase during annealing. This is possible due to the metallic property of the liquid state which produces a readily measured increase in optical reflectivity which can be probed by a low-power continuous HeNe laser. As seen in the upper left trace of Fig. 1, the infrared pulse was not by itself able to melt the sample in

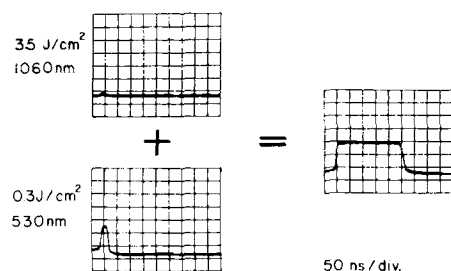


FIG. 1. Time-resolved reflectivity traces showing the duration of the liquid silicon phase for exposure to optical pulses at 1060 and 530 nm. The combination of the two pulses is seen to have a much greater effect than either alone.

spite of its relatively high energy density of 3.5 J cm<sup>-2</sup>. The harmonic pulse, of only 0.3 J/cm<sup>2</sup>, readily produced surface melting, as seen in the lower left trace. The duration of the melt was only 20 ns and, as determined by RBS channeling spectra, the corresponding depth of penetration was not sufficient to result in complete single-crystal regrowth from the undamaged substrate. The combination of these same two pulses, however, had a very dramatically improved effect as indicated by the trace on the right-hand side of Fig. 1. The melt lasted for 260 ns, which was more than sufficient to ensure complete recrystallization. The weak visible pulse thus acted as a trigger and enabled efficient utilization of the infrared energy. The anneal was also much more uniform than those obtained with higher-energy infrared pulses alone.

The thresholds for melting at the two wavelengths can be estimated as follows. First, in the case of the visible radiation the absorption depth is very short and the absorbed energy is deposited within a distance which can be estimated by thermal diffusion. This gives the following approximate expression for the melt threshold for using visible pulses:

$$E^{\text{th}} \approx (1 - R)^{-1} C (T_m - T_0) \sqrt{D \tau_p}, \quad (1)$$

where  $R$  is the (solid phase) reflectivity,  $C$  is the heat capacity,  $T_m$  and  $T_0$  the melting and ambient temperatures, respectively,  $D$  is the thermal diffusivity, and  $\tau_p$  is the pulse duration. The derivation of Eq. (1), of course, assumes that  $C$  and  $D$  are independent of temperature. To account for the temperature variation of  $D$  and  $C$ , we use average values (geometric mean) between the ambient and melting temperatures. Using appropriate values for crystalline silicon of  $R = 0.65$ ,  $D = 0.28 \text{ cm}^2/\text{s}$ ,  $C = 1.9 \text{ J/}^\circ\text{K cm}^3$ ,  $T_m = 1650 \text{ }^\circ\text{K}$ , and  $\tau_p = 4 \times 10^{-8} \text{ s}$ , we find  $E^{\text{th}}(530 \text{ nm}) \approx 0.35 \text{ J/cm}^2$ , which agrees remarkably well with the experimental value, in spite of the coarse approximations employed. Unfortunately, the thermal constants of amorphous silicon are not known. Experimentally,<sup>5</sup> the melting threshold at 530 nm of an implanted crystal was found to be approximately two-thirds that of an unimplanted sample, suggesting that either the melting temperature or thermal conductivity or both are somewhat smaller.

At 1060 nm the situation is very different since the crystalline silicon substrate has a band-to-band absorption coefficient of only  $10 \text{ cm}^{-1}$ . Amorphous silicon, however, has an absorption coefficient of approximately  $7 \times 10^3 \text{ cm}^{-1}$  at 1060 nm. For an amorphous layer of thickness  $l$ , we would expect the melting threshold to be greater at 1060 nm than at 530 nm by a factor of approximately

$$\frac{E_{\text{th}}(1060 \text{ nm})}{E_{\text{th}}(530 \text{ nm})} \approx \frac{1}{1 - \exp(-\alpha l)}. \quad (2)$$

For our particular case of interest, in which  $l = 480 \text{ \AA}$ , we would expect this ratio to be approximately 35 : 1. The observed thresholds<sup>5</sup> are in the ratio 18 : 1, suggesting that substrate absorption also contributes at 1060 nm.

If the effect of the implantation on the crystal is slight so that little or no damage results, the dominant absorption mechanisms responsible for melting at 1060 nm are quite

different. The band-to-band absorption of crystalline silicon is not sufficiently strong to account for the observed melting threshold of  $6 \text{ J/cm}^2$  even if the temperature dependence of the band-gap energy is taken into account. We believe that an accurate description of this process requires the inclusion of the effects of free-carrier absorption and Auger recombination<sup>8</sup> as well. If we assume the temperature  $T$  and carrier density  $n$  profiles are not steep so that diffusion can be ignored, the approximate dynamical equations are

$$\frac{\partial I}{\partial z} = C \frac{\partial T}{\partial t} = [\alpha(T) + \sigma n] I, \quad (3)$$

$$\frac{\partial n}{\partial t} = \frac{\alpha(T) I}{\hbar \omega} - \gamma_3 n^3, \quad (4)$$

where  $\sigma$  is the free-carrier absorption cross section,  $\gamma_3$  is the Auger recombination coefficient, and  $I$  is the optical intensity in the crystal. For the case of interest, the effective carrier lifetime will be very short relative to the pulse duration so that a quasi-steady-state approximation for the carrier density can be made. To model the temperature dependence of the band-to-band absorption,  $\alpha(T)$ , we assume

$$\alpha(T) \approx \alpha_0 (T/T_0)^k. \quad (5)$$

Using theoretical estimates of the temperature dependence of the band gap<sup>9</sup> and the approximate ansatz

$$\alpha(T)|_{\hbar\omega} \approx \alpha(T_0)|_{\hbar\omega - \Delta E_g} \quad (6)$$

we estimate  $k \approx 3$ . Equations (3) and (4) can then be integrated for a rectangular pulse of uniform intensity  $I$  and duration  $\tau_p$  to give the result:

$$I^{4/3} = \frac{C T_0}{\sigma \tau_p} \left( \frac{\gamma_3 \hbar \omega}{\alpha_0} \right)^{1/3} \log \left[ \left( \frac{T_m}{T_0} \right) \times \left( \frac{1 + (\sigma/\alpha_0)(\alpha_0 I / \gamma_3 \hbar \omega)^{1/3}}{(T_m/T_0)^3 + (\sigma/\alpha_0)(\alpha_0 I / \gamma_3 \hbar \omega)^{1/3}} \right)^{1/2} \right]. \quad (7)$$

Using  $\sigma = 4 \times 10^{-18} \text{ cm}^2$  and  $\gamma_3 = 4 \times 10^{-31} \text{ cm}^6/\text{s}$  (Ref. 8), we estimate  $I \approx 1.5 \times 10^8 \text{ W/cm}^2$ , corresponding to an incident pulse energy of approximately  $7 \text{ J/cm}^2$  for a pulse duration of 40 ns, in excellent agreement with the measured melting threshold of  $6 \text{ J/cm}^2$ . The corresponding carrier density just before melting is estimated to be  $1.5 \times 10^{20} \text{ cm}^{-3}$  and the carrier lifetime is only 55 ps!

In conclusion, we wish to point out that a dual-wavelength annealing apparatus can have significant technical advantages by causing the incident flux to be absorbed by a strong mechanism. Thus, the incident energy is used most efficiently in the annealing process. Beyond the question of efficiency it should be noted that under conditions where absorption in the sample is initially small and dependent upon nonlinear processes (as for lightly or undamaged Si with a Nd laser) the effects of various spurious surface contaminants (i.e., dust, grease, etc.) may play a major role in triggering the absorption of annealing energy and inhomogeneous results may be expected. The dual-wavelength scheme eliminates this problem. Finally, the triggering radiation being of modest energy content may be conveniently manipulated spatially across the sample surface. It alone and not the higher-energy long-wavelength light will determine those re-

gions where annealing can be achieved. Thus, small device patterns may be conveniently controlled through the dual-wavelength procedures.

The authors are grateful to N.G. Nilsson for discussions and preprints of the recent measurements of the Auger recombination coefficient and free-carrier cross section in silicon. J. Rodgers, R. D'Angelo, and E. Povilonus helped in sample preparation; and P.R. Smith provided technical support. Conversations with C.M. Surko, P. Petroff, and D. Aspnes were helpful.

<sup>1</sup>See, for example, *Laser-solid interactions and laser processing* Boston, 1978 (American Institute of Physics, New York, 1978).

- <sup>2</sup>D.H. Auston, J.A. Golovchenko, P.R. Smith, C.M. Surko, and T.N.C. Venkatesan, *Appl. Phys. Lett.* **33**, 539 (1978); J.S. Williams, W.L. Brown, H.J. Leamy, J.M. Poate, J.W. Rodgers, D. Rousseau, G.A. Rozgonyi, J.A. Shelnett, and T.T. Sheng, *ibid.*, p. 542.  
<sup>3</sup>D.H. Auston, C.M. Surko, T.N.C. Venkatesan, R.E. Slusher, and J.A. Golovchenko, *Appl. Phys. Lett.* **33**, 437 (1978).  
<sup>4</sup>M. Von Allmen, W. Luthy, M.T. Sinegar, and K. Affolter, in Ref. 1.  
<sup>5</sup>D.H. Auston, J.A. Golovchenko, A.L. Simons, C.M. Surko, and T.N.C. Venkatesan (unpublished); Ref. 1.  
<sup>6</sup>K.N. Shvarev, B.A. Baum, and P.V. Gel'd, *Sov. Phys.-Semicond.* **16**, 2111 (1975).  
<sup>7</sup>M.H. Brodsky, R.S. Title, K. Weiser, and G.D. Pettit, *Phys. Rev. B* **1**, 2632 (1970).  
<sup>8</sup>K.G. Svantesson and N.G. Nilsson (unpublished).  
<sup>9</sup>V. Heine and J.A. Van Vechtan, *Phys. Rev. B* **13**, 1622 (1976).

## The effect of dc current bias on sustained oscillations in (Al,Ga)As double-heterostructure lasers

R. W. Dixon and H. R. Beurrier

*Bell Laboratories, Murray Hill, New Jersey 07974*

(Received 11 December 1978; accepted for publication 16 February 1979)

Sustained oscillations in proton-bombardment-delineated stripe-geometry (Al,Ga)As double-heterostructure injection lasers are shown to be adversely influenced (enhanced) by the presence of dc current bias in the devices. The time constant for this enhancement is found to be in the range 2–5  $\mu$ sec and is interpreted as being thermal in origin. A previously proposed saturable absorber model of pulsations is qualitatively consistent with these results.

PACS numbers: 42.55.Px, 42.80.Sa, 85.60.Jb

One of the most puzzling features of injection lasers is the tendency for their optical outputs to exhibit sustained oscillations (pulsations) either as initially fabricated or after small amounts of aging.<sup>1</sup> These oscillations are of practical concern, in addition to being theoretically interesting, because they occur in frequency ranges (roughly 200–2000 MHz) which interfere with the use of lasers in high-frequency fiber-optic communications applications of the type which are now being extensively investigated throughout the world. Various explanations of these pulsations have been proposed, including saturable absorber *Q*-switching,<sup>2</sup> second-order mode locking,<sup>3</sup> and various mode competition effects.<sup>4</sup> In spite of this work, the causes of pulsations in modern double-heterostructure lasers remain uncertain, and information about their origins is much desired.

In this paper, evidence is presented which we interpret as showing the rather surprising result that *thermal* effects typically make important modifications in the behavior of pulsing lasers and in the associated relaxation oscillations which sometimes exist in the light output following stepped current excitation. Thus, we conclude that thermal effects must be included in any satisfactory explanation of pulsations, and we briefly discuss a previously proposed model in which they may be accommodated.<sup>5</sup>

Consider the optical output shown in Fig. 1(a). It was

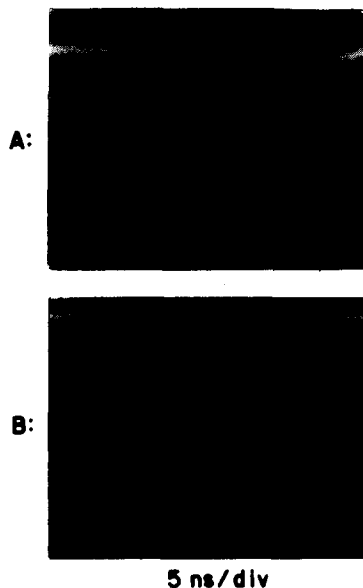


FIG. 1. Light output from an unaged (Al,Ga)As double-heterostructure laser which showed sustained oscillations. In trace A the laser was operated with a current pulse of about 30-nsec duration. Note the high-frequency, not fully developed, oscillations. In trace B the same laser was operated with a dc current bias set just below threshold, with a small amplitude current pulse superimposed. Note the lower-frequency, more fully developed oscillations. (The nominal lasing threshold was 100 mA. In each trace the instantaneous current was adjusted to be 5 mA above threshold.)